Supporting Information For

High-Resolution Hyperpolarized In Vivo Metabolic ^{13}C Spectroscopy at Low Magnetic Field (48.7 mT) Following Murine Tail-Vein Injection

Aaron M. Coffey,[a,b,*] Matthew A. Feldman,[a,b] Roman V. Shchepin,[a,b] Danila A. Barskiy,[a,b] Milton L. Truong,[a,b] Wellington Pham[a,b,c,d] and Eduard Y. Chekmenev[a,b,c,d,e,*]

[a]Vanderbilt University Institute of Imaging Science (VUIIS), [b]Department of Radiology, [c]Department of Biomedical Engineering, [d]Vanderbilt-Ingram Cancer Center (VICC), Vanderbilt University, Nashville, Tennessee 37232-2310, United States

[e]Russian Academy of Sciences, Leninskiy Prospekt 14, Moscow, 119991, Russia

Table of Contents

1. Time Series ^{13}C NMR Spectra Processed with SVD De-Noising

Serial acquisition of a time series of small flip angle (FA=18.2°) ^{13}C NMR spectra permitted pursuing de-noising the signal and thereby increasing SNR via singular value decomposition. Here, the largest singular values possessing the largest information content of the signal, assuming that noise was random, were selected. As seen in Figures S1 and S2, this naïve but easily applied selection criteria indeed results in higher SNR (*Cf* Figure S2, raw NMR spectrum to the SVD spectrum), but does not discriminate against large noise components in the data (see spikes more visible in Figure S1, right).

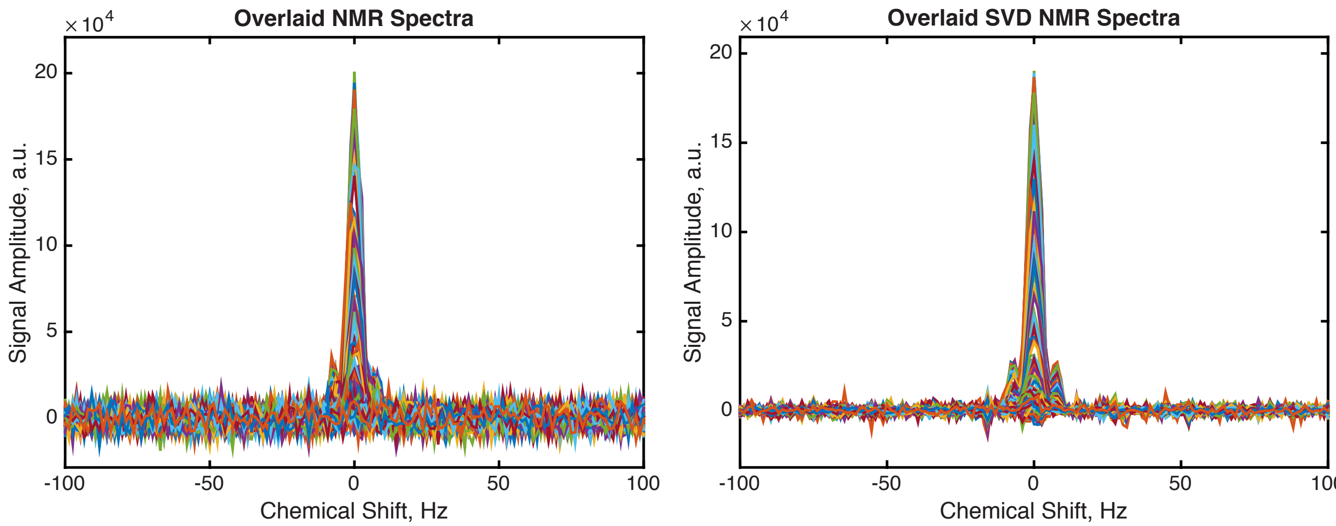

Figure S1. *In vivo* ^{13}C-SUX NMR spectroscopy at low magnetic field. (left) Overlay of all ^{13}C NMR acquisitions (right) Overlay of the SVD of the NMR spectra retaining the 10 most significant singular values.

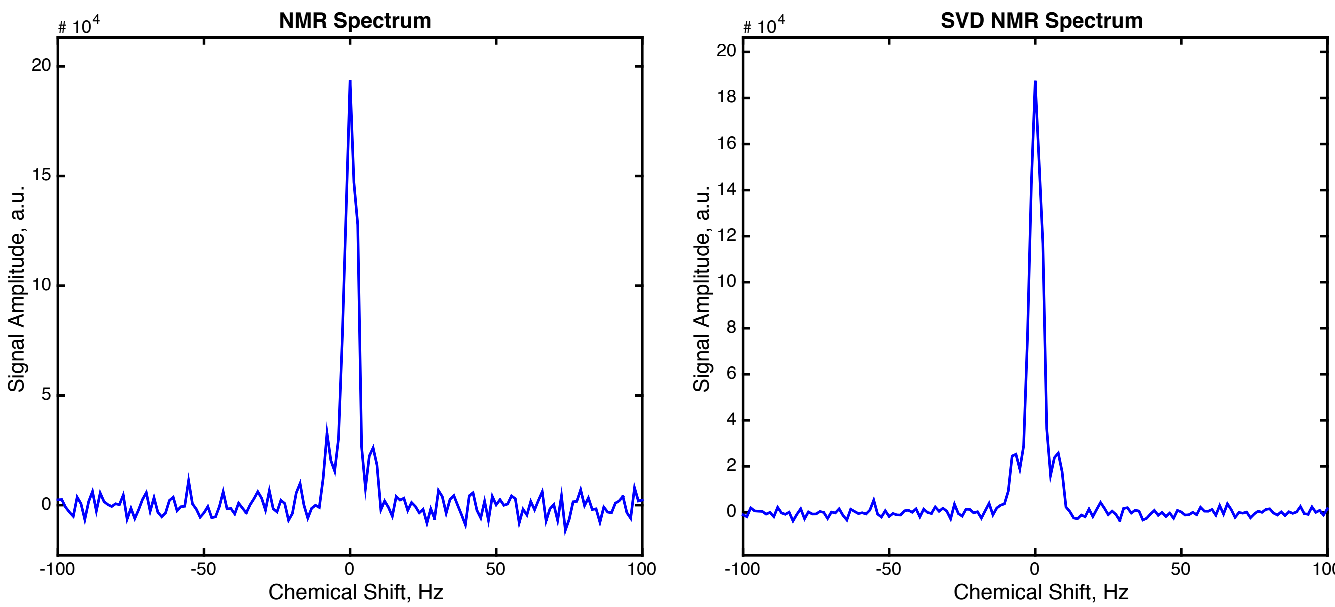

Figure S2. Figure 2 main text selected NMR spectrum. (left) Original acquired NMR spectrum selected from time series. (right) The NMR spectrum with SVD applied to the time series to remove noise at the cost of reduced resolution. The selected SVD NMR spectrum from the time series retains the 10 most significant singular values.

2. Vertical Biplanar Permanent Magnet Clinical Imaging System

Our low-field MRI system operates at 0.0487 Tesla. The static B_0 field is established using neodymium permanent magnets arranged in a vertically oriented, C-shaped open bore configuration with an 80 cm gap width between the gradient coil faces (SIGWA 0.0487 T, Boston NMR, Boston, MA). As installed, the statically B_0 field homogeneity is just under 13 ppm (12.7 as shimmed) measured peak to peak over a 400 mm diameter spherical volume (DSV) for the FOV as measured according to a 24 angle x 25 plane high resolution field map over the spherical surface. For protons with a gyromagnetic ratio of 42.576 MHz/T, this corresponds to a full width half maximum (FWHM) linewidth of ~27 Hz at the proton resonance frequency of B_1=2.074 MHz without application of the XYZ gradients for shimming purposes. Heteronuclear experiments involving ^{13}C and ^{15}N on this system have been observed to approach ~1 Hz linewidths when measuring NMR samples with μL volumes (e.g. samples in 5 mm NMR tubes). We note that this system is particularly well suited for the NMR measurement of *J*-couplings of hyperpolarized compounds given its low field strength and excellent field homogeneity. While not utilized for shimming in the *in vivo* study undertaken and presented in the Main Text, when used for MRI the XYZ planar gradient coil set is capable of reaching 20 mT/m in all axes.

The RF pulse amplifiers (PA) and gradient pulse amplifiers (GPA) for this clinical system are controlled and operated via a Tecmag Redstone console, which is configured with three receiver and transmitter channels. The system is configured to operate across a 0.1-3MHz bandwidth (owing to the use of 0.01-3 MHz RF PA from Tomco Technologies, Stepney, Australia, and a lower frequency bound of 100 kHz for the Redstone receive channels as configured), which allows for future flexibility in studies involving nitrogen-15 labeled contrast agents at B_1=210 kHz, especially as produced via the Para-Hydrogen Induced Polarization (PHIP) or Signal-Amplification By Reversible Exchange (SABRE) hyperpolarization techniques. The nominal noise figure of the receivers is 1.5 dB, which could be improved upon through purchase of more expensive, lower noise figure preamplifiers if it should prove necessary in the future.

3. Configurable ^1H or ^{13}C Resonance RF Probe Design and Calibration

The RF coil built for use in this imaging system was designed to measure metabolic HP contrast agents *in vivo* in small animal studies involving mice. The solenoid coil was constructed to match the typical dimensions of the animal (17 mm diameter by up to 193 mm body length) to increase the coil filling factor and correspondingly the SNR. The coil had a quality factor of 55. The coil was tuned using 56H02 Johansen trimmer capacitors and ATC nonmagnetic ceramic capacitors to tune the resonant frequency and match the coil impedance to the 50 Ω coaxial transmission line impedance. All component values are provided in Tables S1 and S2. The resonant circuit for ^1H or ^{13}C detection was comprised of a parallel LC resonator with a series capacitive matching element (see Figure S3 and S4). The solenoid was constructed with 170 windings using 28 AWG gauge magnet wire with a measured inductance of 302 μH. In the interest of time, no investigation was made to optimize the efficiency of the detection coil to achieve maximum SNR; therefore, the coil's good performance could be a lower bound. For example, all coil windings were wound directly adjacent to their nearest neighbors, which is known to maximize the turn count at the cost of maximizing the effective coil resistance due to the proximity effect, when alternate (but time-consuming) winding geometries can overcome this.[1] Additionally, the close proximity between windings induces an effective parasitic capacitance in parallel with the inductor, which limits the achievable number of windings owing to lowering of the coil self-resonance frequency, which can again be mitigated through use of more advanced winding geometry. [1] The required component values for capacitively tuning and matching to the ^1H and ^{13}C resonance frequencies (Tables S1 and S2) were calculated from the Eq. 1 for the complex impedance of the resonant circuit (see Figures S3 and S4).[2]

$$Z = r + i\,\frac{L(C_p+C_m+C_t)\omega^2-1}{\omega C_m(L(C_p+C_t)\omega^2-1} \qquad \text{(Eq. 1)}$$

The coil was calibrated via a nutation sequence on the Redstone console using variable flip angle via pulse length calibration for fixed power, and the 90° tip angle was determined to be 115 μs for ^{1}H and 475 μs for ^{13}C for <1 W of applied RF power. Since the imaging system is currently not shielded from electromagnetic interference, a shield was constructed for the coil. The shield was constructed using square double-sided 1 oz. copper clad PCB materials to form an enclosed cubic volume (1ft × 1ft × 1ft). The eight exterior edges of the cube were soldered with the final plate serving as a removable lid was conductively connected to the shield using copper tape with a conductive adhesive for ease of use. This shielding provided an electric field suppression of 60 dB and an SNR of 47.4 dB when measuring a 38 mm DSV of H_2O. Future shielding design for the full imaging system will be implemented to enable low field magnetic resonance imaging for biomedical studies.

Coil Windings (turns)	170
Coil Inductance (μH)	302
Parasitic Capacitance (pF)	627
Matching Capacitance (pF)	(122+33+33) || (47+20) + (1-30) = 49.39 + (1-30 variable)
Tuning Capacitance (pF)	(1-30 variable)
Resonant Frequency (MHz)	2.074

Table S1. RF resonator component values for ^{1}H resonance.

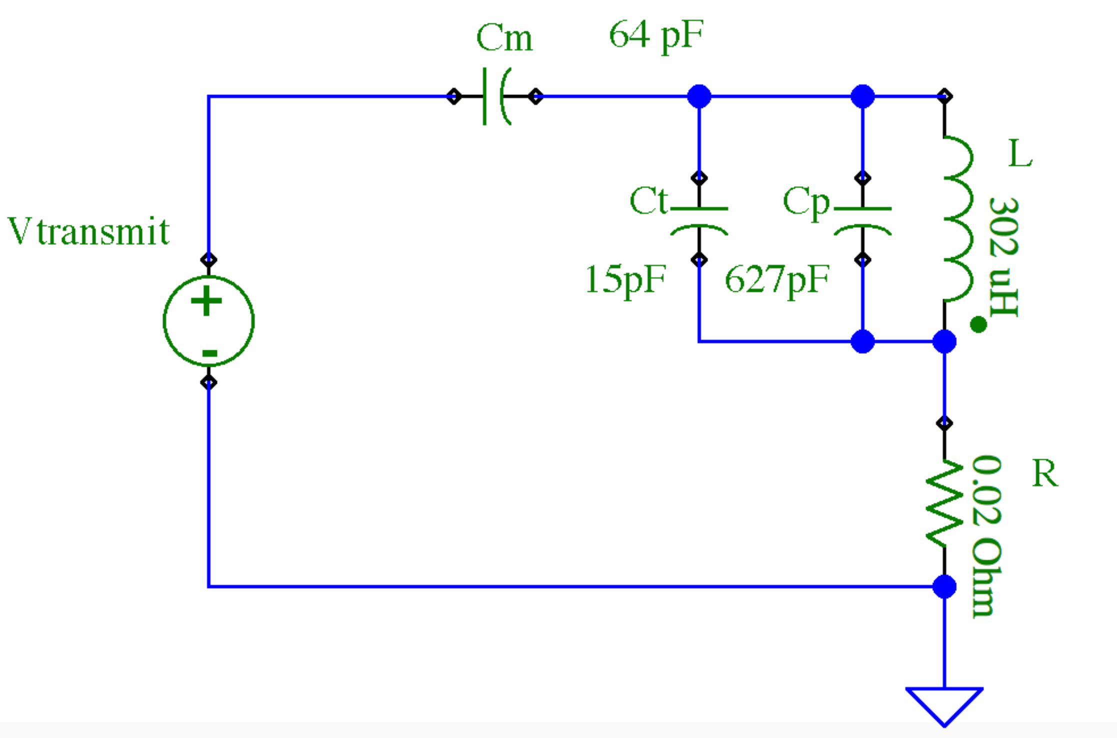

Figure S3. ^{1}H RF resonant circuit with aggregate component values depicted.

Coil Windings (turns)	170
Coil Inductance (µH)	302
Parasitic Capacitance (pF)	11800
Matching Capacitance (pF)	(47+47+33+33) + (1-30) = 160
Tuning Capacitance (pF)	(270+270+39) || (470+470+47) + (1-30) = 414.39 + (1-30)
Resonant Frequency (MHz)	0.52

Table S2. RF resonator component values for ^{13}C resonance.

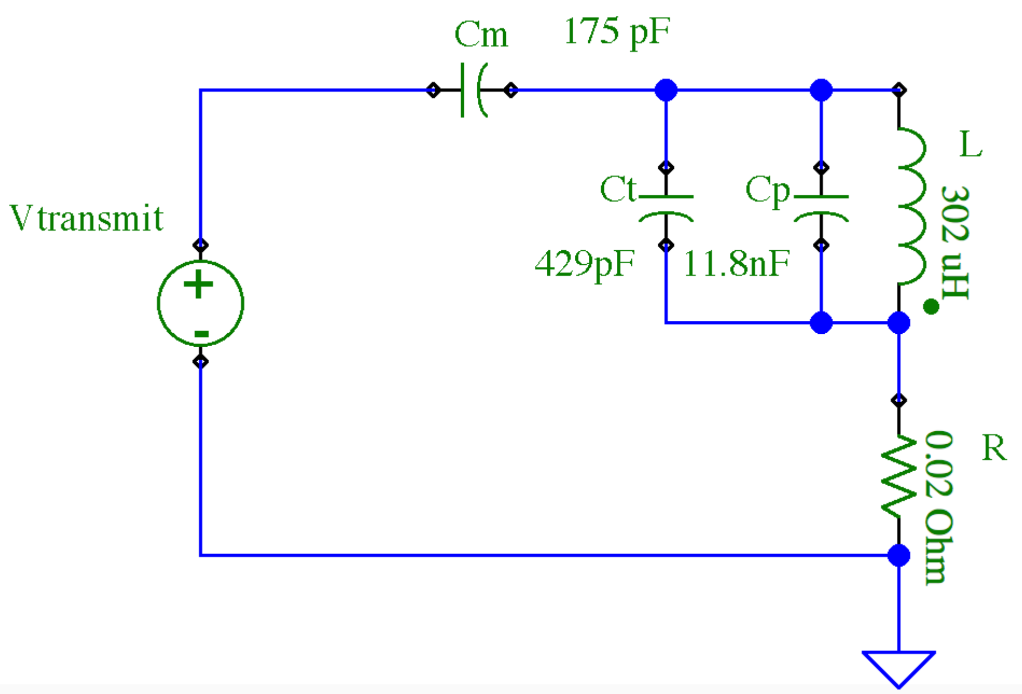

Figure S4. ^{13}C RF resonant circuit with aggregate component values depicted.

4. References Used in Supporting Information

1. Coffey, A.M., Truong, M.L. & Chekmenev, E.Y. Low-field MRI can be more sensitive than high-field MRI. *J Magn Reson* **237**, 169-174 (2013).
2. Mispelter, J.Ã., Lupu, M. & Briguet, A.Ã. *NMR Probeheads for Biophysical and Biomedical Experiments: Theoretical Principles and Practical Guidelines*, (World Scientific Publishing Company Pte Limited, 2015).